Solar Wind Plasma Properties During Ortho-Parker IMF Conditions and Associated Magnetosheath Mirror Instability Response

V. Génot[1] & B. Lavraud[1,2]
1. Institut de Recherche en Astrophysique et Planétologie, CNRS, Université de Toulouse, CNES, Toulouse, France
2. Laboratoire d'Astrophysique de Bordeaux, Université Bordeaux, CNRS, Pessac, France

Paper: https://doi.org/10.3389/fspas.2021.710851

The properties of the solar wind fraction that exhibits an Interplanetary Magnetic Field (IMF) orientation orthogonal to the classical Parker spiral (so-called ortho-Parker) are investigated. We make use of a solar wind plasma categorization scheme, using 10 years of OMNI data, and show that the fractions of the different plasma origins (streamer-belt-origin plasma, coronal-hole-origin plasma, sector-reversal-region plasma and ejecta) identified by this scheme are rather constant when expressed as a function of the IMF orientation whereas the Alfvén Mach number significantly depends on this orientation. This has direct implication on the magnetosheath dynamics and, as an example, the stability of the mirror mode in this compressed plasma is studied thanks to Rankine-Hugoniot anisotropic relations. This study sheds light on previously reported, yet unexplained, observations of a larger occurrence of mirror mode in the magnetosheath downstream of ortho-Parker IMF.

Magnetic field orientation

$$\Phi_P = \arctan_2\left(\frac{-\Omega R}{v_{sw}}\right)$$

$$\Phi_B = \arctan_2\left(B_y/B_x\right)$$

- Φ_B is the azimuthal angle for the observed field
- Φ_P =135° is for a 'nominal' Parker spiral at L1 in the plane $(XY)_{GSE}$

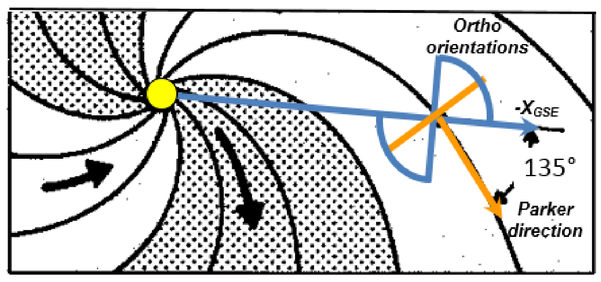

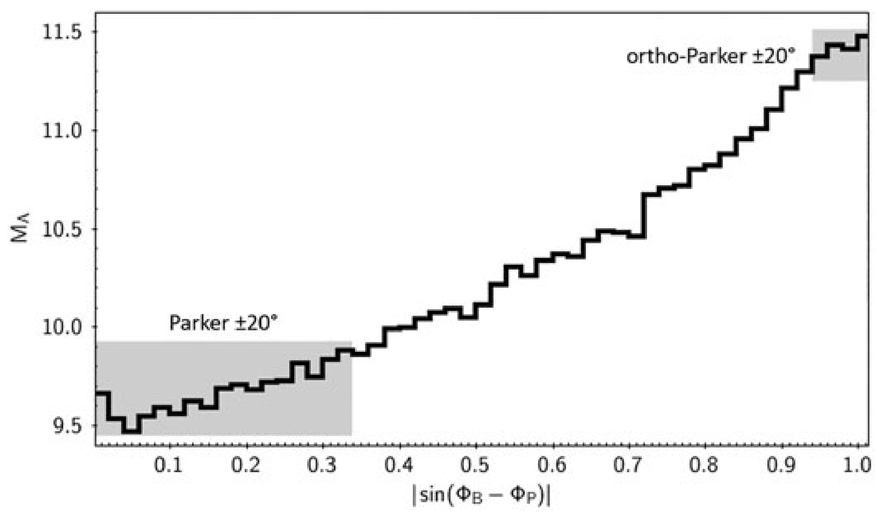

FIGURE 1. Average of the Mach Alfvén number per bin of $|\sin(\Phi_B - \Phi_P)|$. Parker orientations ± 20° are shown in the grey box on the left and the ortho-Parker orientations ± 20° are shown in the upper right grey box.

FIGURE 3. Fractions of the different solar wind populations (**SRR**, **SBO**, **CHO**, and **ejecta**) as a function of $|\sin(\Phi_B - \Phi_P)|$. Parker orientations are to the left and ortho-Parker orientations ± 35° are identified by the grey box to the right.

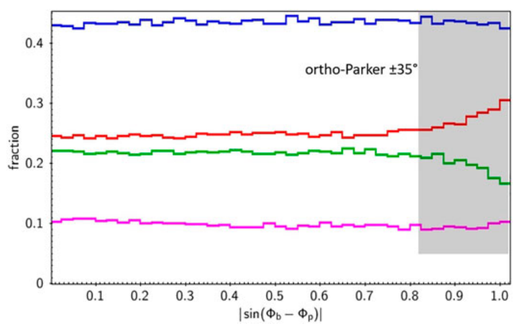

FIGURE 4. Fractions of the different solar wind populations (**SRR**, **SBO**, **CHO** and **ejecta**) as a function of M_A.

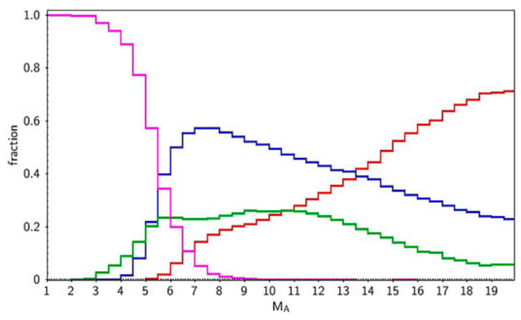

Solar wind characterization

Xu & Borovsky, 2015 https://doi.org/10.1002/2014JA020412

- Streamer belt origin plasma (SBO)
  - Q1 > 1 and Q2 < 1 and Q3 > 1
- Coronal hole origin plasma (CHO)
  - Q1 < 1 and Q2 > 1
- Sector reversal region plasma (SRR)
  - Q1 < 1 and Q3 < 1
- Ejecta : Q1 > 1

$$Q_1 = 0.841 B n_p^{-0.315} T_p^{-0.222} v_{SW}^{-0.171}$$

$$Q_2 = 8.77 \times 10^{-11} T_p B^{1.42} v_{SW}^{3.44} n_p^{-2.12}$$

$$Q_3 = 0.0561 T_p B^{0.752} v_{SW}^{0.445} n_p^{-1.14}$$

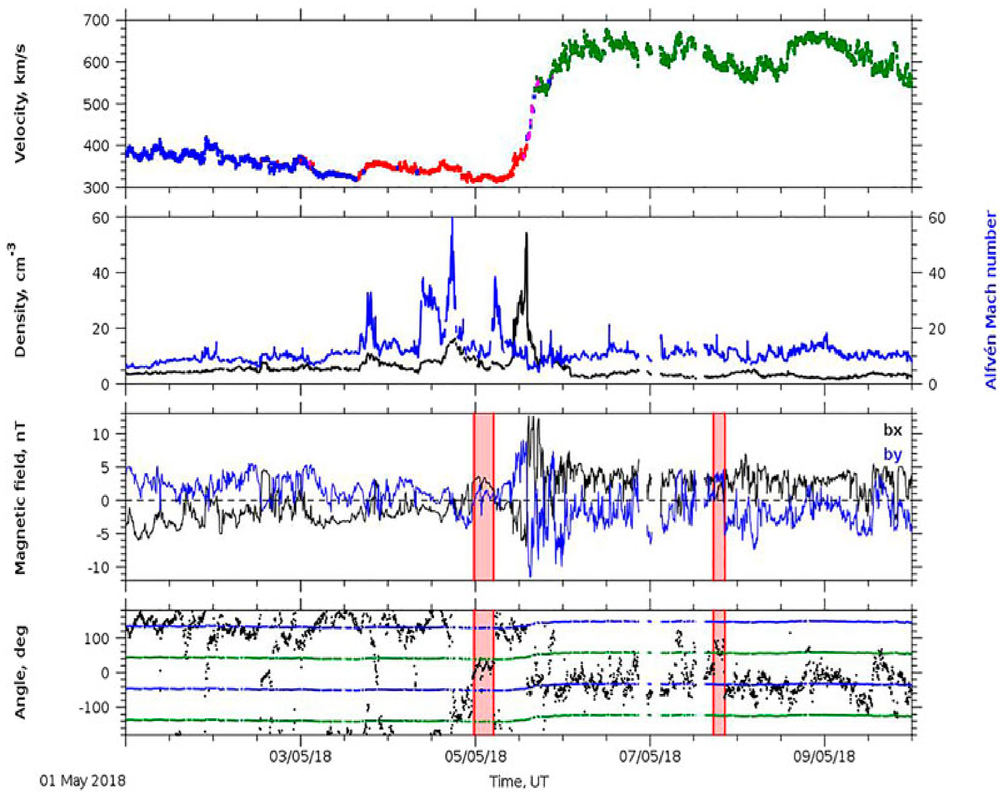

FIGURE 2. 9 days of solar wind in May 2018 observed at L1. The top panel shows the wind velocity colored by the plasma origins: **SRR**, **SBO**, **CHO**, and **ejecta**. The second panel shows the density, which peaks at the "**ejecta**" event seen on the first panel, and the Alfvén Mach number (in blue) which shows high values for **SRR** plasmas. The magnetic field components *bx* (black) and *by* (blue) in GSE are plotted on the third panel. The dotted values on the fourth panel is Φ_B (the observed orientation of the magnetic field), the upper blue line corresponds to Φ_P (the common Parker spiral orientation), the bottom blue line to Φ_P-180° (the so-called anti-Parker orientation), the upper green line to Φ_P-90° (ortho-Parker orientation), and the bottom green line to Φ_P-270° (ortho-Parker orientation). Two examples of prolonged intervals (several hours) of ortho-Parker orientations are shaded red in between thick vertical red lines.

Magnetosheath response

For a perpendicular shock and isotropic solar wind (A_1=1), the magnetosheath parameters are determined from the Rankine-Hugoniot relations:

$$\beta_{\perp 2} = \frac{\beta_1 + 1}{r_s^2} - 1 + \frac{2M_A^2}{r_s^2}\left(1 - \frac{1}{r_s}\right)$$

$$A_2 = \left[\beta_1 + 2M_A^2\left(1 - \frac{1}{r_s}\right) + 1 - r_s^2\right] \times \left[\beta_1 (5r_s - 4) + 2M_A^2\left(r_s + \frac{3}{r_s} - 4\right) + 4(r_s - 1)\right]^{-1}$$

With r_s the magnetic field ratio between the downstream magnetosheath field (B_2) and the upstream/IMF (B_1); this ratio is in the range [1,4]. $A=T_\perp/T_{//}$ is the temperature anisotropy.

FIGURE 6. Same as Fig. 5 but for magnetosheath ***data*** associated to their incident solar wind conditions. We made used of a framework developed by B. Michotte de Welle, N. Aunai, G. Nguyen (LPP). ***See the oral presentation by B. Michotte de Welle and the poster by A. Ghisalberti***. This framework uses machine learning to automatically detect and gather all time intervals of magnetosheath measurements from Cluster, Double Star, THEMIS and MMS missions, and to position each individual measurements relative to regression models of the magnetopause and shock boundaries parametrized by upstream solar wind/IMF parameters. It produced a dataset of 45 million local magnetosheath 5 seconds averaged measurements, in all possible IMF orientations.

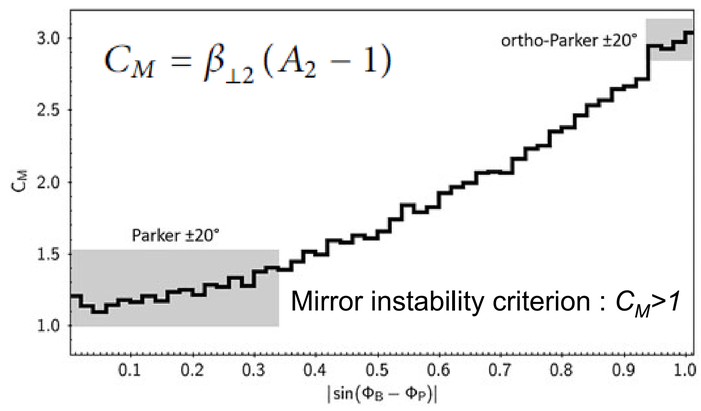

FIGURE 5. Median of the threshold C_M per bin of $|\sin(\Phi_B - \Phi_P)|$ (for a perpendicular shock with r_s = 3.5). Parker orientations ± 20° are shown in the grey box on the left and the ortho-Parker orientations ± 20° are shown in the upper right grey box.

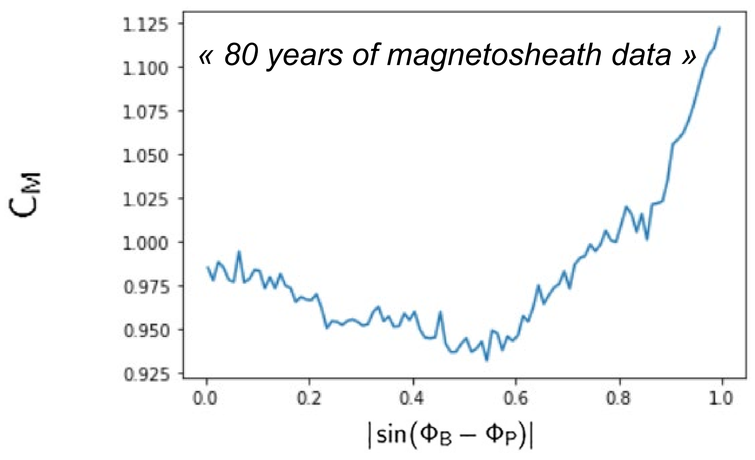

Colloque du Programme National Soleil Terre, Marseille, 16-20 mai 2022